PHYSICAL REVIEW B **69**, 201309(R) (2004)

Real-time scanning tunneling microscopy observation of the evolution of Ge quantum dots on nanopatterned Si(001) surfaces

P. D. Szkutnik,[1,*] A. Sgarlata,[1] S. Nufris,[1] N. Motta,[2] and A. Balzarotti[1]
[1]*Dipartimento di Fisica, Università di Roma Tor Vergata, Via della Ricerca Scientifica 1, I-00133 Roma, Italy*
[2]*Dipartimento di Fisica, Università di Roma Tre, Via della Vasca Navale 84, I-00146 Roma, Italy*
(Received 3 November 2003; revised manuscript received 5 February 2004; published 26 May 2004)

To investigate the effect of surface patterning on island growth, a real-time study by scanning tunneling microscopy (STM) of Ge deposition on nanostructured Si(001) surfaces is presented. The substrate is nanopatterned by the STM tip and the subsequent evolution of a Ge layer deposited at 500 °C is recorded. The formation of the wetting layer, a transition stage and the growth of three-dimensional (3D) Ge huts are examined dynamically. The 2D-3D transition is described in terms of the nucleation and evolution of pre-pyramids consisting of (001) oriented terraces, which eventually transform into pyramids by successive introduction of {105} facets. Substrate patterning strongly affects the positioning of 3D islands, and represents a route toward ordering of Ge islands.

DOI: 10.1103/PhysRevB.69.201309 PACS number(s): 68.47.Fg, 68.37.Ef, 68.55.−a

The assembly of ordered nanostructures on semiconductor IV–IV surfaces is a subject of active experimental and theoretical research.[1–5] The interest derives from the complex nature of the nucleation and self-organization of three-dimensional (3D) quantum dots in SiGe systems.[6–9] Great efforts have been devoted to elucidate island nucleation and growth processes. Mo *et al.*,[10] Vailionis *et al.*[11] and Tersoff *et al.*[5] have observed the existence of embryos before the formation of Ge hut clusters and Voigtländer[9] has examined the metastable nature of these embryos and the asymmetric evolution of the resulting pyramids. Moreover, to order 3D islands, a few lithographic techniques[12–14] have been recently developed.

In this paper, a real time study of Ge deposition on Si(001) substrates patterned by using the tip of the scanning tunneling microscope is presented. The experimental observations provide insight into the wetting layer (WL) formation in presence of a regular array of pits. The evolution of a specific hut from WL to pyramid is followed confirming the existence of a pre-pyramid stage, which evolves with the progressive insertion of {105} facets. Moreover, the results suggest that arrays of intentionally produced pits drive the nucleation process at selected sites. A model based on step interaction is applied to estimate the influence of a pit on the pre-pyramid.

The Si(001) substrate (p type, $\rho = 0.1-0.5\ \Omega$ cm), was annealed by dc heating at 1250°C in ultrahigh vacuum to obtain a clean (2×1) reconstructed surface. Then, at 500°C, the sample was nanopatterned by using scanning tunneling microscopy (STM) lithography. At selected positions, with the z-feedback switched-off, pits were elaborated by approaching the STM tip to the surface. The resulting regular array was re-imaged by the same tungsten tip during the next scan. Pits have diameters ranging from 8 to 15 nm and depths of 1–2 monolayers (ML) and the distance between them is 60 ± 5 nm. Before deposition, the stability of the array was assessed by a long annealing process (30 min). On the nanopatterned surface, the growth of Ge at 500°C by physical vapor deposition was recorded in real-time by STM. In this kind of experiment a tip shadowing effect[9] occurs causing a lower growth rate in the scanned area. The Ge coverage is estimated from the increasing area of terraces between two successive images during the layer-by-layer growth. A Ge flux of $(2.6\pm0.3)\times10^{-3}$ ML/s was evaluated and kept constant.

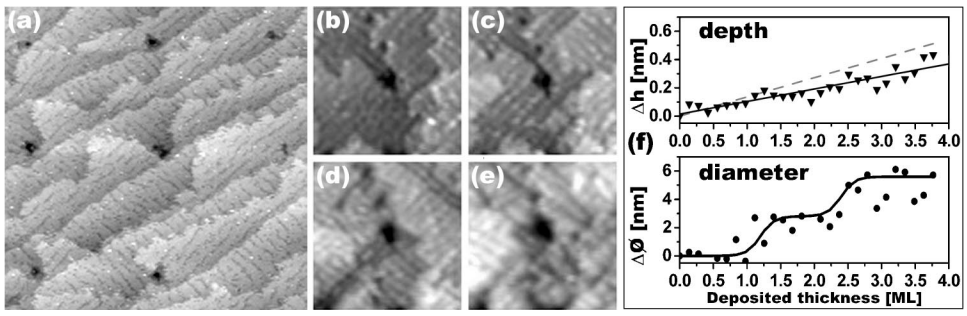

FIG. 1. Real-time images of the wetting layer on a nanostructured Si(001) surface. (a) STM image $(150\times150\times2)$ nm^3 of an array of pits elaborated with the STM tip after deposition of 0.2 ML of Ge, (b)–(e) STM images $(50\times50\times0.5)$ nm^3 of the surface during Ge deposition at 500°C for coverages of: (b) 0.87 ML, (c) 0.99 ML, (d) 1.24 ML, (e) 1.48 ML, (f) Pits' depth Δh and diameter $\Delta\varnothing$ changes with coverage. Closed points correspond to experimental data, full lines to fits. The dashed line gives the thickness variation of the deposited Ge layer with coverage.

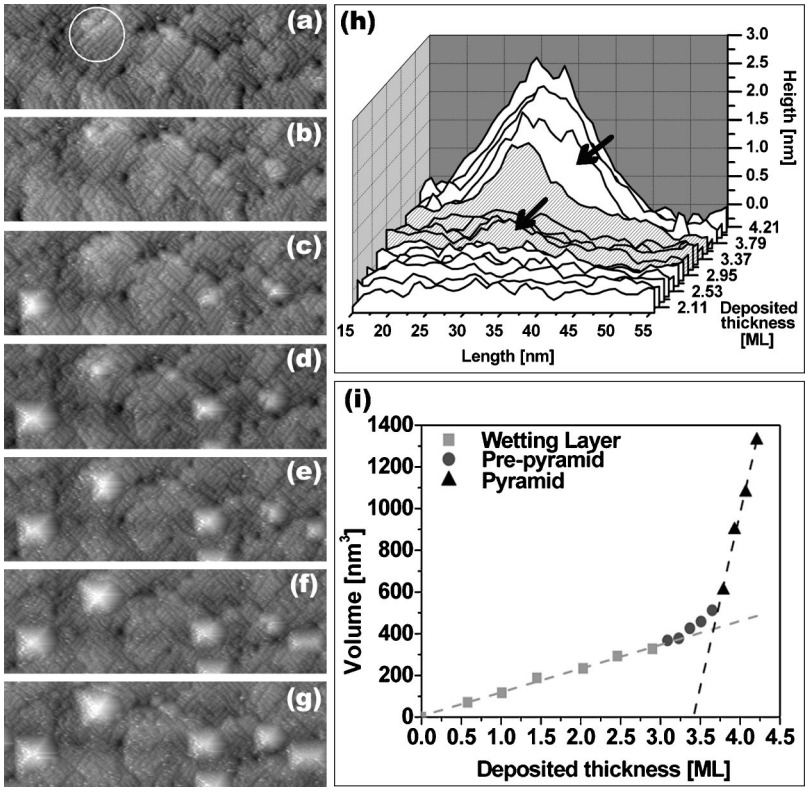

FIG. 2. Real-time growth of pyramids on a nanostructured Si(001) surface. (a)–(g) STM images $(250\times80\times3)$ nm^3 extracted from the movie of Ge deposition at 500°C for coverage of: (a) 3.23 ML, (b) 3.37 ML, (c) 3.51 ML, (d) 3.65 ML, (e) 3.79 ML, (f) 3.93 ML, (g) 4.07 ML. (h) Evolution of the profile of the hut cluster (circled) vs coverage. The arrows mark the initial step of formation of a pre-pyramid and of a pyramid. (i) Evolution of the volume of the hut cluster (circled) as a function of coverage. Experimental data refer to the volume of the WL (squares), pre-pyramids (dots) and pyramids (triangles); the dashed lines are the corresponding fits.

Figure 1(a) shows a nanopatterned Si(001) surface after 0.2 ML of Ge deposited. Figures 1(b)–1(e) display four images extracted from an STM movie of Ge growth. At the beginning a step flow process occurs meaning that the WL forms on the step edge enlarging the terraces. It appears that the WL encloses the pits that are not filled up by Ge, and increases the surface roughness. The analysis of this sequence is represented in Fig. 1(f) by the evolution of the pits' depth and diameter changes as a function of Ge coverage, θ. To understand the growth mechanism of Ge atoms with respect to the pits, the sign of the ''depth rate'' (DR), defined as the slope of the fitted pit depth, is analyzed. For a positive DR value, the pit depth increases, implying that more Ge atoms attach outside than inside the pit. The limit case, in which no Ge atoms fall inside the pit, corresponds to the increment of one-layer height for each deposited layer, that is DR$=0.136$ nm/ML. In the present case the fit provides a value of DR$=0.09\pm0.01$ nm/ML indicating that a few Ge atoms go inside the pit. However, data analysis confirms that they do not fill the pit. The plot of pits diameter changes in Fig. 1(f) provides information about the localization of Ge atoms. A constant diameter means that the WL ends at the border of the pit. Here, the diameter increases jumping every 1.15 ML of Ge coverage.[15] A good fit to the experimental data is obtained using a step function with 2.8 nm jumps which gives an equilibrium distance of 1.4 ± 0.3 nm between the step edges of two adjacent layers. This distance fits the space needed to host a $p(2\times2)$ or $c(4\times2)$ reconstructed unit cell. So the new growing layers form an angle of $5.5\pm0.2°$ with the surface, close to 6°, the critical angle reported by Sutter *et al.*[16]

The 2D-3D transition takes place between 3 and 4 ML of Ge coverage. The real-time growth of a Ge hut cluster [circled in Fig. 2(a)] is shown in Figs. 2(a)–2(g). In this sequence, two different states can be identified: the first stage corresponds to a pre-pyramid (at $\theta=3.23$ ML), while the second one to a pyramidal hut (at $\theta=3.79$ ML). Additional information is obtained by plotting the 3D line profile [Fig. 2(h)] of the ''circled'' cluster as a function of coverage. Between 2.11 and 2.95 ML, the profile illustrates the WL formation. At $\theta=3.23$ ML, a new structure which grows laterally is distinguishable [arrowed in Fig. 2(h) and circled in Fig. 2(a)] and corresponds to a two-layer-high platelet. Then, successive small layers form upon it reaching a height of 0.8 nm. The corresponding line profile shows a very clear transition to the characteristic shape of a hut cluster. At $\theta=3.79$ ML, a complete square base pyramid is observed which grows by developing its four {105} facets.[10,17] This is apparent on the line profiles from 3.79 to 4.21 ML, which have triangular shapes with constant slope but height and base progressively increasing. The height-to-width ratio varies between 0.015 and 0.03 in good agreement with that measured by Vailionis *et al.*[11] and reaches 0.1, when the transition to a pyramid is completed [gray area in Fig. 2(h)].

Quantitative information on the growth mechanism can be obtained from the volume of the hut as a function of θ depicted in Fig. 2(i). The volume is measured on a selected and fixed area[18] which is flat at $\theta=0$ ML and displays a fourfold pyramid at $\theta=4.21$ ML. In Fig. 2(i) three regimes are distinguishable and identified, on the basis of STM images, as WL, 2D-3D transition and pyramid growth. The first regime, ($\theta=0-3$ ML), is fitted by a linear function whose coefficient of 114 nm^3/ML depends on the size of the chosen area. By normalizing this coefficient to the unit area, the value of

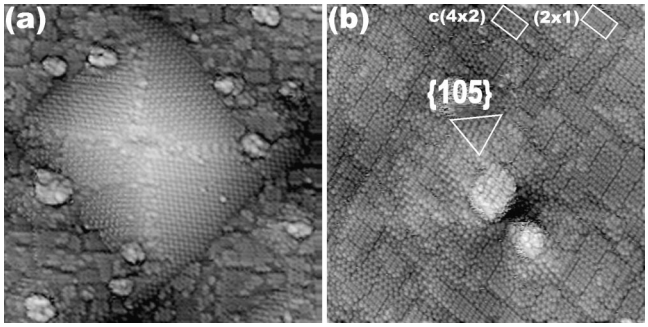

FIG. 3. STM images of different clusters on a Si(001) surface. (a) STM image ($60\times60\times3.5$) nm^3 of a pyramidal hut cluster at 9 ML of Ge coverage, (b) STM image ($50\times50\times3$) nm^3 of the pre-pyramid after 3.5 ML of Ge coverage showing the (2×1) and $c(4\times2)$ reconstruction and a {105} domain.

0.13 nm/ML is obtained, demonstrating the layer-by-layer growth mode of the WL. Similarly, in the third regime, $\theta = 3.79–4.21$ ML, the pyramid growth exhibits a linear behavior.[19] Since the shape of the cluster is compatible with a regular pyramid, see Fig. 3(a), whose volume is proportional to L^3, the linear dependence on coverage demonstrates that the pyramid grows by enlarging its base side L. This is interpreted as a layer-by-layer growth occurring specifically on the facets of the pyramid.[21,22] In this case, the larger rate of change of 1670 nm^3/ML indicates that the growth of the pyramid requires more atoms than those deposited on the selected area. As the Ge flux is constant and no depletion region is observed around the hut, a germination process has to take place. Specifically, Ge atoms diffuse toward the pyramid from a collection (Voronoi) area larger than that initially selected. This area, assumed to be a square, has a side of 95 nm as evaluated from the ratio of the slopes of the first and third regimes. Hence, a density of the 3D clusters of 1.1×10^{10} cm^{-2} is calculated comparable to that of 3×10^{10} cm^{-2} obtained from STM images. The two linear fits cross at $\theta=3.66$ ML, indicating that the material accumulated during the WL growth is enough to generate a hut cluster by a rearrangement of its initial structure.[11] However, as the volume deviates from these fits in the second regime, the growth of a pre-pyramid is assumed. Between 3 and 3.79 ML, a transition region occurs characterized in Fig. 3(b) by the coexistence of (2×1) and $c(4\times2)$ reconstructed domains and a {105} incomplete facets. According to Fig. 2(i) and to STM images, the experimental evidence suggests that a first layer forms on the WL corresponding to the base of the future pyramid. Then, by increasing θ, new layers grow on top of each other. These overlapping layers extend until forming an energetically favored {105} facet.[23] The coalescence of disconnected {105} domains leads to the formation of a pyramid facet and eventually to a hut cluster.

The volume of the pre-pyramid as a function of coverage can be expressed by

$$V(\theta)=\frac{X}{4}\times V_P+\left(1-\frac{X}{4}\right)\times V_{\mathrm{WL}}(\theta), \qquad (1)$$

where V_{WL} is the volume of the overlapping layers, equal to that of the WL, and $0\leqslant X\leqslant 4$ is the fraction of a {105} facet. V_P,[24] equal to 542 nm^3, is defined as the volume of the pyramid just after the 2D-3D transition. Computed volumes are obtained from Eq. (1) for different values of X and for θ corresponding to experimental coverages. Good agreement between calculated and experimental volumes is found for integer values of X. This means that, during the transition, the system evolves as a pre-pyramid composed progressively of one ($X=1$), two ($X=2$), or three ($X=3$) complete {105} facets. The presence of a critical nucleus of stepped shape which evolves up to the appearance of {105} facets is also suggested by Sutter and Lagally[25] but they do not specify if all facets appear simultaneously. Furthermore, our volume data can be also fitted by the model of Tersoff *et al.*[5] considering a constant base side of 14 nm and a base angle continuously increasing up to 11°. However, this model does not explain the presence of partial {105} facets.

Considering the lateral arrangement, it is remarkable that a pre-pyramid always nucleates around a pit. To evaluate the relaxation energy originating from elastic interactions between islands and pits, the system is modeled [Fig. 4(a)] by a stepped island (with steps of equal spacing s) adjacent to a four-layer deep square pit. The elastic relaxation energy ΔG_r relative to that of the pit is[26,27]

$$\Delta G_r = A\sum_{i\neq j}\mathrm{sign}(i)\mathrm{sign}(j)(x_i-x_j)\ln\left(\frac{x_i-x_j}{a}\right), \qquad (2)$$

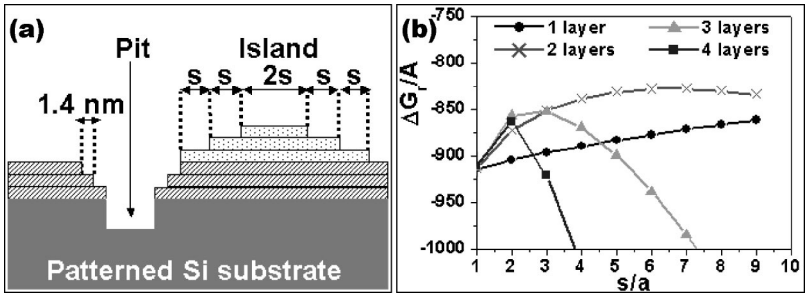

FIG. 4. Calculated relaxation energy for a pre-pyramid near a pit using the one-dimensional elastic interaction model described by Eq. (2) of the text. (a) Cross-sectional schematic representation of a pit plus wetting layer and a three-layer high island considered for the calculation. (b) Evolution of the normalized relaxation energy, $\Delta G_{r,}/A$ as a function of the step width s for an island one- to four-layers high. $A=C\sigma^2h^2$, where σ is the bulk stress of the epilayer, h is the step height and $C=(1-\nu)/(2\pi\mu)$ is the misfit stress where μ is the shear modulus and ν is the Poisson's ratio.

where A is a constant, sign$=\pm 1$ counts the attractive $(+)$ or repulsive $(-)$ monopole interactions between two steps with the same or opposite orientation, respectively, $x_i - x_j$ is the distance between the i and j steps and a is a cutoff length of the order of the lattice parameter of Ge. In Fig. 4(b), $\Delta G_r/A$ is plotted as a function of s/a for different numbers of layers forming the island. For a one-layer high island, the growth is unlikely, while two-layer high pre-pyramids have increasing relaxation magnitude for $s/a > 8$ and thus high probability to grow. For a square-base pre-pyramid a width of 16 nm and an aspect ratio of 0.017 are calculated, consistent with the experiment. With the same reasoning, by increasing the height from two to four layers, smaller size pre-pyramids can nucleate near the pit. In general, the localization of pre-pyramids is driven by the local chemical potential which contains two contributions. The relaxation of the strain energy selects small pits as nucleation sites[27] (near the pit) while the curvature term is important for large pits.[4,28]

In summary, Ge growth on nanopatterned Si(001) surfaces at 500 °C has been followed in real time by STM. During the WL formation, Ge atoms do not go inside the pits. Rather, they form new layers which stop at 1.4 nm from the pit boundary. As a consequence, the pits diameter and depth increase with coverage. The growth of a pre-pyramid is characterized by the combination of {105} faceting and stepped morphology. When all parts of a facet are connected, the pyramid grows by developing its four facets. On nanopatterned surfaces, pits act as preferential sites for the nucleation of pre-pyramids. From these results, it appears that STM nanolithography can be exploited to form ordered arrays of Ge islands by choosing a periodic array of pits and taking into account the diffusion of Ge atoms over the collection area.

The authors acknowledge illuminating discussions with M. Fanfoni. This work was supported by the European Community (EC) through FORUM-FIB contract (IST-2000-29573) and partially by INFM.

*Corresponding author; electronic address: Szkutnik@roma2.infn.it

[1] L. Vescan, T. Stoica, B. Holländer, A. Nassiopoulou, A. Olzierski, I. Raptis, and E. Sutter, Appl. Phys. Lett. **82**, 3517 (2003).
[2] F. Patella, A. Sgarlata, F. Arciprete, S. Nufris, P. D. Szkutnik, E. Placidi, M. Fanfoni, N. Motta, and A. Balzarotti, J. Phys.: Condens. Matter **16**, S1503 (2004).
[3] A. Sgarlata, P. D. Szkutnik, A. Balzarotti, N. Motta, and F. Rosei, Appl. Phys. Lett. **83**, 4002 (2003).
[4] M. Borgstrom, V. Zela, and W. Seifert, Nanotechnology **14**, 264 (2003).
[5] J. Tersoff, B. J. Spencer, A. Rastelli, and H. Von Känel, Phys. Rev. Lett. **89**, 196104 (2002).
[6] I. Berbezier, A. Ronda, and A. Portavoce, J. Phys.: Condens. Matter **14**, 8283 (2002).
[7] C. Teichert, Phys. Rep. **365**, 335 (2002).
[8] T. I. Kamins, G. Medeiros-Ribeiro, D. A. A. Ohlberg, and R. S. Williams, J. Appl. Phys. **85**, 1159 (1999).
[9] B. Voigtländer, Surf. Sci. Rep. **43**, 127 (2001).
[10] Y.-W. Mo, D. E. Savage, B. S. Swartzentruber, and M. G. Lagally, Phys. Rev. Lett. **65**, 1020 (1990).
[11] A. Vailionis, B. Cho, G. Glass, P. Desjardins, D. G. Cahill, and J. E. Greene, Phys. Rev. Lett. **85**, 3672 (2000).
[12] M. Kammler, R. Hull, M. C. Reuter, and F. M. Ross, Appl. Phys. Lett. **82**, 1093 (2003).
[13] L. Vescan, K. Grimm, M. Goryll, and B. Hollander, Mater. Sci. Eng., B **69–70**, 324 (2000).
[14] P. D. Szkutnik, D. Sander, F. Dulot, F. A. d'Avitaya, and M. Hanbücken, J. Vac. Sci. Technol. B **20**, 960 (2002).
[15] The absence of the jump, at a coverage of 3.45 ML, indicates that the effect is linked to the step configuration and occurs only during the layer-by-layer growth.
[16] P. Sutter, P. Zahl, and E. Sutter, Appl. Phys. Lett. **82**, 3454 (2003).
[17] P. Raiteri, D. B. Migas, L. Miglio, A. Rastelli, and H. Von Känel, Phys. Rev. Lett. **88**, 256103 (2002).
[18] The selected area where nucleation takes place is smaller than the Voronoi's area of the pyramid but allows a better estimation of the volume.
[19] According to the linear evolution of the pyramid's volume, Floro *et al.* (Ref. 20) report that the linear behavior of the volume of the pyramids changes toward the hut-to-dome transition.
[20] J. A. Floro, G. A. Lucadamo, E. Chason, L. B. Freund, M. Sinclair, R. D. Twesten, and R. Q. Hwang, Phys. Rev. Lett. **80**, 4717 (1998).
[21] D. E. Jesson, G. Chen, K. M. Chen, and S. J. Pennycook, Phys. Rev. Lett. **80**, 5156 (1998).
[22] M. Kästner and B. Voigtländer, Phys. Rev. Lett. **82**, 2745 (1999).
[23] P. Sutter, I. Schick, W. Ernst, and E. Sutter, Phys. Rev. Lett. **91**, 176102 (2003).
[24] V_P is estimated from Eq. (1) assuming that at 3.65 ML, where the volume is 512 nm^3, the pre-pyramid has three reconstructed and one unreconstructed {105} facet.
[25] P. Sutter and M. G. Lagally, Phys. Rev. Lett. **84**, 4637 (2000).
[26] J. Tersoff, Phys. Rev. Lett. **74**, 4962 (1995).
[27] D. E. Jesson, M. Kästner, and B. Voitgländer, Phys. Rev. Lett. **84**, 330 (2000).
[28] T. Schwarz-Selinger, Y. L. Foo, D. G. Cahill, and J. E. Greene, Phys. Rev. B **65**, 125317 (2002).